

# Molecular structure of tin(II) acetate as determined in the gas phase by electron diffraction and *ab initio* calculations

Bruce A. Smart, Lucy E. Griffiths, Colin R. Pulham, Heather E. Robertson,  
Norbert W. Mitzel and David W. H. Rankin\*

Department of Chemistry, University of Edinburgh, West Mains Road, Edinburgh EH9 3JJ, UK

The gas-phase structure of tin(II) acetate,  $\text{Sn}(\text{O}_2\text{CCH}_3)_2$ , has been determined by electron diffraction augmented by flexible restraints derived from *ab initio* molecular orbital calculations at the DZ(P)/MP2 level. The structure, with  $C_2$  symmetry, can be regarded as a highly distorted trigonal bipyramid, with the lone pair of electrons on tin occupying one of the equatorial sites. The four-membered rings and the acetate groups were both found to adopt near-planar arrangements. The two equivalent acetate groups are asymmetrically bonded to tin, with  $\text{Sn}-\text{O}(4)$  233.7(12) and  $\text{Sn}-\text{O}(5)$  219.2(8) pm, and form a narrow bite angle at tin, with  $\text{O}(4)-\text{Sn}-\text{O}(5)$   $58.1(2)^\circ$ ; other important experimental structural parameters ( $r_e$ ) are  $\text{C}(2)-\text{O}(4)$  124.5(5),  $\text{C}(2)-\text{O}(5)$  127.5(5) and  $\text{C}(2)-\text{C}(8)$  151.0(5) pm,  $\text{C}(2)-\text{Sn}-\text{C}(3)$   $95.1(12)^\circ$ ,  $\text{O}(4)-\text{C}(2)-\text{O}(5)$   $122.0(4)^\circ$  and  $\text{O}(4)-\text{Sn}-\text{C}(2)-\text{O}(5)$   $176.3(16)^\circ$  and the acetate groups are twisted about the  $\text{Sn} \cdots \text{C}$  axis by  $16.8(11)^\circ$  away from a rhomboidal-based pyramid.

As part of a programme to investigate methods for the production of nanophase metal oxides, we have recently studied the suitability of tin(II) acetate,  $\text{Sn}(\text{O}_2\text{CCH}_3)_2$ , as a precursor to small particles of tin(II) oxide. Details of this work will be reported elsewhere.<sup>1</sup> Although tin(II) acetate was first prepared in 1882,<sup>2</sup> very little structural information is available for the compound in either the solid or gas phase. An X-ray powder diffraction study showed that the material contains eight molecules in an orthorhombic unit cell, but attempts to grow single crystals were unsuccessful.<sup>3</sup> The compound's low solubility in non-polar solvents suggested that a polymeric structure is adopted in the solid phase,<sup>3</sup> but the infrared spectrum provided no conclusive evidence for this.<sup>4</sup> As the solid can be sublimed *in vacuo* at 420 K we have undertaken a structural study by gas-phase electron diffraction (GED). Under the conditions required for tin(II) oxide particle formation the compound is present in the gas phase and so knowledge of the structure in this phase is of fundamental importance in gaining an understanding of the mechanism of decomposition to the oxide. As far as we are aware, this study also represents the first structural characterisation of a tin(II) carboxylate.

As part of our on-going research directed towards improved structural analysis, electron diffraction data for tin(II) acetate have been combined with information derived from *ab initio* calculations according to the SARACEN (structure analysis restrained by *ab initio* calculations for electron diffraction) method.<sup>5</sup> Additional geometrical and vibrational information, which were calculated *ab initio*, were entered in the refinement procedure as predicate observations. Therefore the final structure has been determined from both experimental and theoretical information, and is as reliable as possible at present.

## Experimental

### Synthesis of tin(II) acetate

Tin(II) acetate was prepared by refluxing tin(II) oxide and 50% v/v acetic acid under nitrogen.<sup>3</sup> After filtration and evaporation, the white powder was dried *in vacuo* over sodium hydroxide before being purified by vacuum sublimation at 413–418 K and collected at 308–313 K. The purity of the compound was checked by reference to its infrared spectrum.<sup>4</sup> The electron impact (EI) mass spectrum showed no peaks at  $m/z > 244$  and so suggests that the predominant species in the gas phase is monomeric tin(II) acetate. A mass spectrum also showed that

under the conditions of the electron-diffraction measurements there is no significant decomposition to acetone and carbon dioxide, and this is corroborated by the observation that the sample remained white, with no decomposition to black tin(II) oxide.

### Theoretical methods

All calculations were performed on a Dec Alpha 1000 4/200 workstation using the GAUSSIAN 94 program.<sup>6</sup> Geometries and frequencies were calculated from analytic first and second derivatives, respectively. Preliminary calculations on tin(II) acetate were performed in  $C_1$  symmetry using the 3-21G\*<sup>7-9</sup> basis set at the self-consistent field (SCF) level. To investigate structures with and without an active lone pair of electrons, arrangements with geometries near to a tetrahedron, trigonal bipyramid and square pyramid were considered. All structures collapsed to a distorted trigonal bipyramid possessing overall  $C_2$  symmetry. More extensive calculations were undertaken at both the SCF and second-order Møller-Plesset perturbation (MP2) levels of theory employing a larger basis of double zeta quality with polarization functions on all non-hydrogen atoms [DZ(P)]; this comprised a 15s,11p,7d/11s,7p,4d basis set for tin<sup>10</sup> combined with the 9s,5p/4s,2p and 4s/2p basis of Dunning and Hay<sup>11</sup> for first-row atoms and hydrogen and supplemented with a single set of d-type polarisation functions for all non-hydrogen atoms [exponents 0.18 (Sn), 0.85 (O) and 0.75 (C)].

Vibrational-frequency calculations were performed at the 3-21G\*/SCF and DZ(P)/SCF level for tin(II) acetate to verify that the structure represents a local minimum on the potential-energy surface and for the calculation of vibrational amplitudes to assist in the refinement of electron-diffraction data.

### Electron diffraction measurements

Electron scattering intensities were recorded on Kodak Electron Image plates using the Edinburgh gas-diffraction apparatus operating at ca. 44.5 kV (electron wavelength ca. 5.7 pm).<sup>12</sup> Nozzle-to-plate distances for the metal inlet nozzle were 201.5 and 257.9 mm yielding data in the range  $s$  20–224 nm<sup>-1</sup>; four and three plates were exposed at the short and medium camera distances, respectively. The sample and nozzle temperatures were maintained at 493 K during the exposure periods.

**Table 1** Nozzle-to-plate distances (mm), weighting functions ( $\text{nm}^{-1}$ ), correlation parameters, scale factors and electron wavelengths (pm) used in the electron diffraction study

Nozzle-to-plate distance <sup>a</sup>	257.89	201.49
$\Delta S$	2	4
$S_{\min}$	20	40
$SW_1$	40	60
$SW_2$	140	192
$S_{\max}$	164	224
Correlation parameter	0.434	0.212
Scale factor <sup>b</sup>	0.899(14)	0.705(13)
Electron wavelength	5.653	5.654

<sup>a</sup> Determined by reference to the scattering pattern of benzene. <sup>b</sup> Values in parentheses are estimated standard deviations.

**Table 2** GED structural parameters for  $\text{Sn}(\text{O}_2\text{CCH}_3)_2^*$

(a) Independent parameters

$p_1$ Sn–O (mean)	226.4(5)
$p_2$ Sn–O (difference)	14.5(19)
$p_3$ C–O (mean)	126.0(2)
$p_4$ C–O (difference)	3.0(10)
$p_5$ C(2)–C(8)	151.0(5)
$p_6$ C–H (mean)	112.1(10)
$p_7$ Sn $\cdots$ C(2)	258.6(7)

$p_8$ C(2) $\cdots$ Sn $\cdots$ C(3)	95.1(13)
$p_9$ C–C–H (mean)	111.6(11)
$p_{10}$ C–CH <sub>3</sub> tilt	13(2)
$p_{11}$ C–CH <sub>3</sub> rock	–2(3)
$p_{12}$ O <sub>2</sub> tilt	–1.1(4)
$p_{13}$ $\tau(\text{O}_2\text{CCH}_3)$	16.8(11)
$p_{14}$ $\tau(\text{CH}_3)$	1.0 (fixed)
$p_{15}$ CH <sub>3</sub> tilt	1.3 (fixed)

(b) Dependent parameters

$p_{16}$ O(4)–Sn–O(5)	58.1(2)
$p_{17}$ O(4)–Sn–O(6)	121(4)
$p_{18}$ O(4)–Sn–O(7)	80(4)
$p_{19}$ O(5)–Sn–O(7)	90(3)
$p_{20}$ Sn–O(4)–C(2)	86.2(6)
$p_{21}$ Sn–O(5)–C(2)	93.5(4)
$p_{22}$ O(4)–C(2)–O(5)	122.0(4)
$p_{23}$ O(4)–C(2)–C(8)	120(3)
$p_{24}$ O(5)–C(2)–C(8)	117(3)
$p_{25}$ O(4)–Sn–C(2)–O(5)	176.3(16)

\* Distances in pm, angles in  $^\circ$ . For definitions of parameters, see text. Values in parentheses are the estimated standard deviations.

The scattering patterns of benzene were also recorded for the purpose of calibration; these were analysed in exactly the same way as for tin(II) acetate so as to minimise systematic errors in the wavelengths and camera distances. Nozzle-to-plate distances, weighting functions used to set up the off-diagonal weight matrix, correlation parameters, final scale factors and electron wavelengths for the measurements are collected in Table 1.

The electron-scattering patterns were converted into digital form using a computer-controlled Joyce Loeb MDM6 microdensitometer with a scanning program described elsewhere.<sup>13</sup> The programs used for data reduction<sup>13</sup> and least-squares refinement<sup>14</sup> have been described previously; the complex scattering factors were those listed by Ross *et al.*<sup>15</sup>

### Molecular model

On the basis of the *ab initio* calculations detailed below, the model used to define the atomic coordinates of tin(II) acetate was constrained to have overall  $C_2$  symmetry with local  $C_3$  symmetry assumed for CH<sub>3</sub> groups. The structure was defined by a total of 15 independent geometrical parameters, compris-

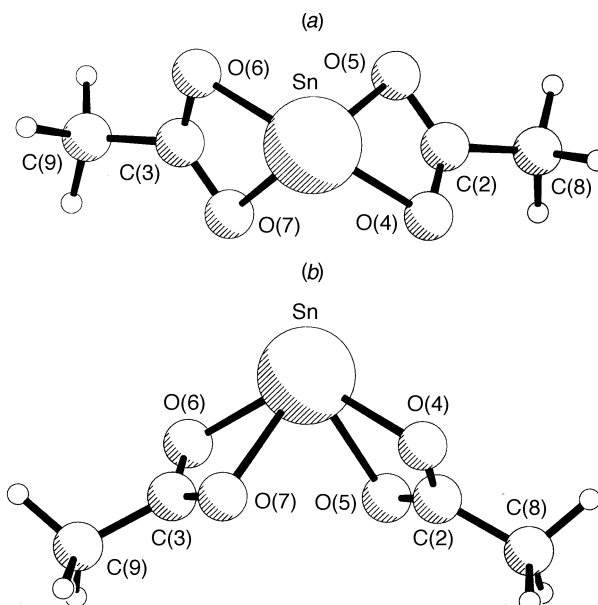


**Fig. 1** Molecular geometry of tin(II) acetate, viewed (a) along the  $C_2$  axis, (b) perpendicular to the  $C_2$  axis

ing seven distance and eight angle parameters (see Table 2). The distances consisted of the average Sn–O bond length,  $p_1$ , the difference between non-equivalent Sn–O bond lengths,  $p_2$ , the mean and difference of the C–O bond lengths,  $p_3$  and  $p_4$ , the bond lengths C–C,  $p_5$ , and C–H,  $p_6$ , and the Sn  $\cdots$  C cross-ring non-bonded distance,  $p_7$ . The eight angles included the C  $\cdots$  Sn  $\cdots$  C angle,  $p_8$ , and the average C–C–H bond angle,  $p_9$ . The six remaining angle parameters were defined relative to an initially planar  $\text{SnO}_2\text{C}$  ring lying in the  $x$ - $y$  plane with the Sn(1)  $\cdots$  C(2) vector lying on the  $y$  axis with the carbon atom at the origin. Parameters  $p_{10}$  and  $p_{11}$  are distortions of the C–CH<sub>3</sub> groups in the  $y$ - $z$  and  $x$ - $y$  planes, respectively, such that  $p_{10}$  is a rotation of the C–CH<sub>3</sub> unit about the  $x$  axis which is followed by an equivalent rotation,  $p_{11}$  about the  $z$  axis. The parameter  $p_{12}$  is the dihedral angle between the O, Sn, O and O, C, O planes;  $p_{13}$  is the rotation of the acetate groups anticlockwise about its Sn  $\cdots$  C axis relative to starting positions in which both the O, Sn, O planes were parallel to the  $x$  axis and perpendicular to the C, Sn, C plane. The final parameters are  $p_{14}$ , the twist of the methyl group clockwise about the C(2)–C(8) bond away from a starting position with one H atom in the  $y$ - $z$  plane and in the negative  $z$  direction, and  $p_{15}$ , which is the tilt angle between the  $C_3$  axis of the methyl hydrogens and the C(2)–C(8) bond.

## Results

### *Ab initio* calculations

Four possible starting structures for tin(II) acetate were considered. Arrangements in which the lone pair of electrons is sterically active and ones which it is inactive were included and, for both cases, symmetrically and asymmetrically bonded acetate groups were considered. When geometry optimisations were performed in  $C_1$  symmetry all arrangements collapsed to a structure with overall  $C_2$  symmetry. Calculations predicted that  $\text{Sn}(\text{O}_2\text{CCH}_3)_2$  has a sterically active lone pair of electrons and two equivalent acetate ligands which are highly asymmetric (see Fig. 1). Values of molecular parameters are reported in Table 3.

At the lowest level of theory adopted (3-21G\*/SCF) the two non-equivalent Sn–O bond lengths were predicted to be 231.2 and 211.9 pm, a difference of 19.3 pm. The difference is predicted to be larger (21.4 pm) at the DZ(P)/SCF level, but is reduced to 16.8 pm when the effects of electron correlation are taken into account. At our highest level, DZ(P)/MP2, estimates of the Sn–O bond lengths were 218.4 and 235.2 pm. The highly

**Table 3** Theoretical molecular geometry and energy of tin(II) acetate \*

Parameter	3-21G*/SCF	DZ(P)/SCF	DZ(P)/MP2	GED
Sn–O(4)	231.2	235.9	235.2	233.7(12)
Sn–O(5)	211.9	214.5	218.4	219.2(8)
C(2)–O(4)	125.4	123.6	127.1	124.5(5)
C(2)–O(5)	129.6	127.2	130.1	127.5(5)
C(2)–C(8)	148.9	150.0	150.3	151.0(5)
C(8)–H (mean)	108.1	108.3	109.4	112.1(10)
C(2)–Sn–C(3)	94.6	97.3	96.3	95.1(13)
O(4)–Sn–O(5)	58.0	56.8	58.3	58.1(2)
O(4)–Sn–O(6)	123.3	124.4	123.2	121(4)
O(4)–Sn–O(7)	81.3	83.6	81.8	80(4)
O(5)–Sn–O(7)	88.4	90.0	90.8	90(3)
Sn–O(4)–C(2)	89.5	88.0	88.0	86.2(6)
Sn–O(5)–C(2)	97.3	97.2	94.8	93.5(4)
O(4)–C(2)–O(5)	115.3	118.0	118.8	122.0(4)
O(4)–C(2)–C(8)	124.5	122.9	122.3	120(3)
O(5)–C(2)–C(8)	120.3	119.1	118.9	117(3)
C(2)–C(8)–H (mean)	109.4	109.8	109.3	111.6(11)
$\tau(\text{O}_2\text{CCH}_3)$	20.2	20.0	18.5	16.8(11)
O(4)–Sn–C(2)–O(5)	179.6	178.6	178.2	176.3(16)
Energy/ $E_h$	–6448.728 41	–6477.179 86	–6478.542 11	—

\* Predicted distances ( $r_e$ ) in pm, angles in °;  $E_h \approx 4.36 \times 10^{-18}$  J.

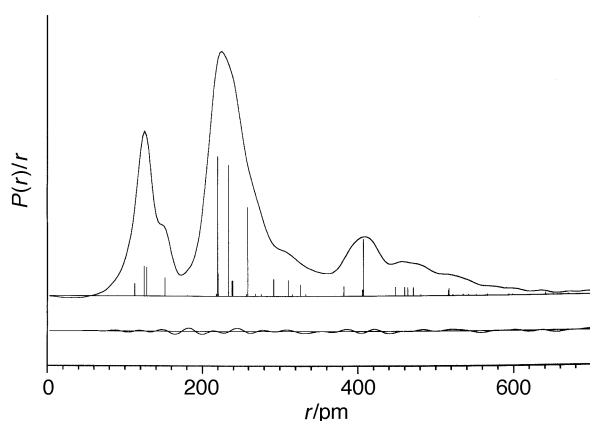


**Fig. 2** Observed and final difference radial distribution curves for tin(II) acetate. Before Fourier inversion the data were multiplied by  $s \exp[-0.00002s^2/(Z_O - f_O)/(Z_{Sn} - f_{Sn})]$

asymmetric bonding of the acetate ligands is also reflected both in the C–O bonds, which were predicted to be 127.1 and 130.1 pm long, and the twist of the acetate groups, 18.5° at the DZ(P)/MP2 level.

The four-membered rings were found to be very nearly planar, with improvements in the level of theory leading to slightly more puckered rings. Our best estimate of the O(4)–Sn–C(2)–O(5) dihedral angle was 178.2° [DZ(P)/MP2]. Similarly, both acetate groups were also predicted to be virtually planar. At all three levels of theory used the sum of angles about the central carbon of the acetate group was found to be 360.0°.

### Electron diffraction refinement

The radial distribution curve for tin(II) acetate (Fig. 2) consists of three distinct peaks at distances of about 125, 225 and 405 pm, plus weaker peaks and shoulders. The peak at 125 pm corresponds to C–O scattering, with a small contribution from the C–H bonds, and a broad shoulder at ca. 150 pm is due to C–C scattering. The most intense peak in the radial distribution curve (225 pm) corresponds to scattering from Sn–O bonds with minor contributions from C···O and O···O non-bonded pairs. The intense shoulder at ca. 260 pm is due to Sn···C cross-ring scattering. The third peak, at 405 pm, con-

sists almost entirely of scattering between tin and the methyl carbon atoms.

The set of starting parameters for the  $r_s$  structure refinement was taken from theoretical geometries optimised at the DZ(P)/MP2 level. The theoretical [DZ(P)/SCF] Cartesian force field was converted into symmetry coordinates using the ASYM 40 program<sup>16</sup> and was scaled to obtain amplitudes of vibration ( $u$ ). Scaling factors were chosen to be 0.95, 0.90 and 0.85 for bond stretches, angle bends and torsions, respectively. The presence of a number of low-frequency vibrational modes led to overestimated predictions of the perpendicular amplitudes of vibration ( $k$ ). Since these values were considered to be unreliable, corrections for shrinkage effects were not included.

The presence of a large number of similar interatomic distances required either the fixing of parameters or the use of flexible restraints (SARACEN method).<sup>5</sup> Six geometric and two vibrational amplitude restraints were used in the refinement procedure. The six geometrical parameters restrained were the difference between Sn–O distances, difference between C–O distances, mean C–H bond length, mean C–C–H bond angle, sum of angles about the central carbon atom of the acetate groups and O(4)–Sn–C(2)–O(5) dihedral angle, which describes the planarity of the four-membered rings. Values were taken to be those predicted at the DZ(P)/MP2 level (see Table 2).

Uncertainties of 2.0 and 1.0 pm were chosen for the difference between the two Sn–O distances and the two C–O distances; the larger uncertainty adopted for the Sn–O difference was chosen to reflect the larger variations in the predicted value of this parameter compared to those for the C–O difference. An uncertainty of 1.5 pm was adopted for the average C–H bond length, while uncertainties of 1.5 and 2° were used for the average C–C–H angle and the O(4)–Sn–C(2)–O(5) angle, respectively.

Additional restraints were applied to the ratio of the two different Sn–O and the two C–O amplitudes of vibration. In each case predicted amplitudes of vibrations were obtained from the scaled SCF force field and the ratio of the two amplitudes adopted as a flexible restraint with an attached uncertainty of 5%. The ratio of the amplitudes of vibration of the two non-equivalent Sn–O bonds was restrained to 0.520(26) : 1 while a ratio of 0.944(47) : 1 for the C–O amplitudes was adopted for GED refinements.

The use of flexible restraints allowed the refinement of 19 independent parameters, comprising 13 geometrical parameters

**Table 4** Interatomic distances ( $r_a$ ) and amplitudes of vibration ( $u$ ) for  $\text{Sn}(\text{O}_2\text{CCH}_3)_2$ 

<i>i</i>	Atoms	Distance ( $d_i$ )	Amplitude ( $u_i$ )
1	Sn–O(4)	233.7(12)	18.9(9)
2	Sn–O(5)	219.2(8)	10.6(5)
3	C(2)–O(4)	124.5(5)	4.5(4)
4	C(2)–O(5)	127.5(5)	4.8(5)
5	C(2)–C(8)	151.0(5)	5.0 <sup>b</sup>
6	C–H	112.1(10)	7.6 <sup>b</sup>
7	Sn...C(2)	258.6(7)	10.2(9)
8	C(2)...O(6)	238(4)	7.2 <sup>b</sup>
9	C(2)...O(7)	239(4)	6.8 <sup>b</sup>
10	O(4)...O(5)	220.4(5)	5.0 <sup>b</sup>
11	O(4)...O(7)	292(13)	19.1 <sup>b</sup>
12	O(4)...O(6)	311(11)	24.5 <sup>b</sup>
13	O(5)...O(7)	406(7)	29.2 <sup>b</sup>
14	C(3)...O(6)	326(11)	24.5 <sup>b</sup>
15	C(3)...O(7)	382(10)	26.2 <sup>b</sup>
16	C(2)...C(9)	382(13)	20.2 <sup>b</sup>
17	Sn...C(8)	407.3(6)	10.9(8)

<sup>a</sup> Distances in pm, angles in °. Values in parentheses are the estimated standard deviations. <sup>b</sup> Fixed.

**Table 5** Correlation matrix ( $\times 100$ ) for parameters of tin(II) acetate\*

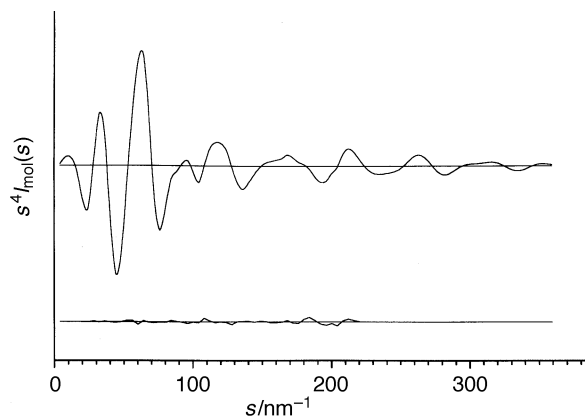
	$p_1$	$p_{10}$	$p_{11}$	$u_2$	$u_3$	$k_1$
$p_1$	56					
$p_{15}$			–67			
$u_1$		–54		61		54
$u_4$					86	
$u_7$		–62				
$k_1$				60		
$k_2$				55		64

\* Only elements with absolute values greater than 50 are shown.

and six amplitudes of vibration. Geometrical parameters  $p_{14}$  and  $p_{15}$ , which define the positions of the hydrogen atoms, were always fixed at the values calculated *ab initio* since little information is contained in the experimental data because of the poor scattering ability of hydrogen. Details of the structural parameters obtained in the optimum refinement are given in Table 2; the corresponding distances and amplitudes are collected in Table 4. The most significant elements of the correlation matrix are presented in Table 5. The success of the final refinement, for which  $R_D = 0.073$ , may be assessed on the basis of the difference between the experimental and calculated radial distribution curves (Fig. 2) while Fig. 3 offers a similar comparison between the experimental and calculated molecular scattering intensity curves.

## Discussion

The SARACEN method has allowed the refinement of all significant parameters leading to a full structure with realistic estimated standard deviations. Overall, good agreement between experiment and theory was obtained for tin(II) acetate despite the different structural types (*i.e.*  $r_a$  vs.  $r_c$ ). Theoretical predictions of bond lengths were generally found to fall within one or two standard deviations of the experimentally determined result. Unexpectedly large deviations occurred in values for the C–O bond distances, where theory predicts bond lengths which are around 2.5 pm longer than the experimentally determined values. This difference is most probably due to limitations in the basis set. Good agreement was also obtained for bond and dihedral angles, although angles about the central carbon of the acetate group are poorly defined by experiment. Surprisingly good agreement between theory and experiment was obtained for O–Sn–O angles since low-frequency twisting modes of the acetate groups [112 (a) and 121  $\text{cm}^{-1}$  (b), DZ(P)/SCF] were expected to lead to substantial vibrational averaging effects.

**Fig. 3** Electron-diffraction molecular scattering intensity and difference curves for tin(II) acetate. A theoretical curve is shown for the regions  $s < 20$  and  $s > 240 \text{ nm}^{-1}$  for which no experimental data were available

The structure of tin(II) acetate is perhaps best described as being based on a distorted trigonal bipyramid in which the longer bonds to O(4) and O(6) occupy axial positions while O(5), O(7) and the lone pair occupy the equatorial positions. The very tight bite angle of the acetate groups imposes considerable distortion from regular trigonal-bipyramidal co-ordination, with angle O(4)–Sn–O(6) 121(4) instead of 180° and O(5)–Sn–O(7) 90(3) instead of 120°. An alternative view of the molecule is obtained if we notice that the four oxygen atoms are almost coplanar and form the base of a rhomboid-based pyramid with side lengths of 220.4(5) pm [O(4)...O(5)] and 292(13) pm [O(4)...O(7)]. This arrangement is strikingly similar to the structural motif adopted in solid tin(II) oxide, in which the tin atom lies above the plane of four oxygen atoms [Sn–O 221(1) pm and O–Sn–O 118(2)°].<sup>17</sup> The  $\text{SnO}_2\text{C}$  rings are virtually planar and it is the twist of these rings through 16.8(11)° that distorts the planar base of the pyramid.

Scope for direct comparison is limited as there are no other tin(II) carboxylates that have been structurally characterised, but structures of some other acetates are available. Tin(IV) acetate features bidentate acetate groups in pseudo-dodecahedral co-ordination in which there is some variation in the Sn–O distances (213–229 pm) ascribed to relief of overcrowding.<sup>18</sup> The acetate groups are asymmetrically bonded to tin and both the acetate groups and the four-membered rings are close to planar. A similar arrangement is found for lead(IV) acetate in which the variation in the Pb–O distances is smaller (224.4–231.2 pm), presumably as the co-ordination sphere around the larger lead atom is less overcrowded.<sup>19</sup> Overcrowding is clearly not the reason for the asymmetric Sn–O distances in tin(II) acetate. Rather it is the nature of the bonding combined with the bite angle of the acetate group that dictates the asymmetry in this case. The structure of tin(II) acetate shows a striking similarity to that of  $[\text{Hg}(\text{O}_2\text{CCH}_3)_2(\text{PBU}_3)]$  in which the two acetate groups are asymmetrically bonded with Hg–O distances of 266 and 225 pm or 258 and 227 pm and equatorial and axial O–Hg–O angles of 90.7 and 125.0°, respectively.<sup>20</sup>

## Acknowledgements

We thank the ESPRC for financial support of the Edinburgh Electron Diffraction Service (grant GR/K44411), for the provision of the microdensitometer facilities at the Daresbury Laboratory and for the Edinburgh *ab initio* facilities (grant GR/K04194). We are grateful to the Royal Society for the provision of a University Research Fellowship (to C. R. P.) and to the European Union for a Marie Curie Fellowship (to N. W. M.).

## References

- 1 L. E. Griffiths, A. Harrison, C. R. Pulham and A. G. Whittaker, unpublished work.
- 2 A. Ditte, *Ann. Chim. Phys.*, 1882, **27**, 115.
- 3 J. D. Donaldson, W. Moser and W.B. Simpson, *J. Chem. Soc.*, 1964, 5942.
- 4 J. D. Donaldson, J. F. Knifton and S. D. Ross, *Spectrochim. Acta*, 1965, **21**, 215.
- 5 A. J. Blake, P. T. Brain, H. Mc Nab, J. Miller, C. A. Morrison, S. Parsons, D. W. H. Rankin, H. E. Robertson and B. A. Smart, *J. Phys. Chem.*, 1996, **100**, 12 280.
- 6 M. J. Frisch, G. W. Trucks, H. B. Schlegel, P. M. W. Gill, B. G. Johnson, M. A. Robb, J. R. Cheesman, T. A. Keith, G. A. Petersson, J. A. Montgomery, K. Raghavachari, M. A. Al-Laham, V. G. Zakrzewski, J. V. Ortiz, J. B. Foresman, J. Cioslowski, B. B. Stefanov, A. Nanayakkara, M. Challacombe, C. Y. Peng, P. Y. Ayala, W. Chen, M. W. Wong, J. L. Andres, E. S. Replogle, R. Gomperts, R. L. Martin, D. J. Fox, J. S. Binkley, D. J. Defrees, J. Baker, J. P. Stewart, M. Head-Gordon, C. Gonzalez and J. A. Pople, GAUSSIAN 94, Revision C.2, Gaussian Inc., Pittsburgh, PA, 1995.
- 7 J. S. Binkley, J. A. Pople and W. J. Hehre, *J. Am. Chem. Soc.*, 1980, **102**, 939.
- 8 M. S. Gordon, J. S. Binkley, J. A. Pople, W. J. Pietro and W. J. Hehre, *J. Am. Chem. Soc.*, 1982, **104**, 2797.
- 9 W. J. Pietro, M. M. Francl, W. J. Hehre, D. J. Defrees, J. A. Pople and J. S. Binkley, *J. Am. Chem. Soc.*, 1982, **104**, 5039.
- 10 T. H. Dunning, unpublished work.
- 11 T. H. Dunning and P. J. Hay, in *Modern Quantum Chemistry*, Plenum, New York, 1976, pp. 1–28.
- 12 C. M. Huntley, G. S. Laurenson and D. W. H. Rankin, *J. Chem. Soc., Dalton Trans.*, 1980, 954.
- 13 S. Cradock, J. Koprowski and D. W. H. Rankin, *J. Mol. Struct.*, 1981, **77**, 113.
- 14 A. S. F. Boyd, G. S. Laurenson and D. W. H. Rankin, *J. Mol. Struct.*, 1981, **71**, 217.
- 15 A. W. Ross, M. Fink and R. Hildebrandt, in *International Tables for Crystallography*, ed. A. J. C. Wilson, Kluwer, Dordrecht, 1992, vol. C, p. 245.
- 16 L. Hedberg and I. M. Mills, *J. Mol. Spectrosc.*, 1993, **160**, 117.
- 17 W. J. Moore and L. Pauling, *J. Am. Chem. Soc.*, 1941, **63**, 1392.
- 18 N. W. Alcock and V. L. Tracy, *Acta Crystallogr., Sect. B.*, 1979, **35**, 80.
- 19 M. Schürmann and F. Huber, *Acta Crystallogr., Sect. C.*, 1994, **50**, 1710.
- 20 P. J. Roberts, G. Ferguson, R. G. Goel, W. O. Ogini and R. J. Restivo, *J. Chem. Soc., Dalton Trans.*, 1978, 253.

Received 12th December 1996; Paper 6/08356K